ACOUSTICS 2012

Pulsed bi-frequency method for characterization of microbubbles in the context of decompression sickness

D. Fouan[a], T. Goursolle[b], P. Lasaygues[a] and S. Mensah[a]

[a]Laboratoire de Mécanique et d'Acoustique, 31, Chemin Joseph Aiguier - 13402 Marseille Cedex 20

[b]BF-systemes, 229, chemin de la Farlède, 83500 La Seyne Sur Mer, France
damien.fouan@bf-systemes.fr

1 Abstract

During hyperbaric decompression, the absolute ambient pressure is reducing; microbubbles may be generated from pre-existing gas nuclei. An accurate monitoring of the size and of the density of the bubble population will provide a valuable means to understand the nucleation and growth processes in tissues. In this aim, an ultrasonic characterization method based on a dual frequency technique applied on a single bubble is tested. The method consists in sending two ultrasonic waves on a stationary bubble. One is a low frequency wave (30 kHz$\leq f_{lf} \leq$60 kHz), which excites the bubble near its resonance frequency and the other is a high frequency (f_{hf}=1MHz) wave that measures the changes in the acoustic cross-section induced by the low frequency activation. The resonance frequency, directly related to the radius, can be detected by looking at the spectrum. The development of an optimal sensor embedded on a diver leads to the use of a single transducer acting as an transmitter/receiver of pulsed waves. The straight forward outcome is a higher probability detection and a better radius estimation accuracy. Distinctions in the signal processing allows dedicated detection/sizing processes suitable either for bubbles circulating in the blood flow (larger bubble) or for stationary bubbles in tissues (several microns).

2 Introduction

Microbubble detection and sizing are a really current issue in many scientific fields. Although detection can be industrially applied, for example in nuclear reactor [1], their most important interest is in the field of medical imaging and diagnostic [2]. Indeed, because of their strong sound scatter effects, bubbles can be used as contrast agent in echography imaging [3]. In this case, gas microbubbles are encapsulated, injected in the patient blood system and the echography contrast is increased with their presence. Encapsulation ensures a longer life-time and a better control of the microbubble size [4]. But microbubbles are not just good acoustic scatterers, they have also an highly nonlinear behaviour. This characteristic is often used in the main ultrasound contrast imaging techniques [3, 5].

Decompression sickness is an other application field where bubble detection and sizing in blood flow is very useful [6]. Indeed, in the beginning of the 1970's, Nishi *et al.* showed the link between diving accident and microemboli appearance [7], [8]. The detection and sizing of such microemboli would be a breakthrough in decompression sickness prevention. Actually the detection is done by hyperbaric doctors on the surface. They use acoustical Doppler systems and estimate the quantity of bubbles thanks to the Spencer grades [9]. This scale allows to assess the risk for the diver. Although some signal treatment techniques are tested in order to do automatic detection [10], the operator dependence is the main drawbacks of this method. Moreover, there is no information about the size of the bubbles detected and the doctor can't make the difference between a single bubble and a group of several bubbles. The capabilities of precise counting the quantity of bubbles and giving an idea of their size is an opportunity to ensure more security to the divers. The different wellknown techniques to size bubbles are mainly based on the non linear behaviour. Leigthon has made a comparison between eight different techniques [11] like for example second harmonic scattering [12], subharmonic scattering [13] or combined techniques [14]. The dual frequency mixing method is one of their [15]. It is based on the link between bubble resonance frequency and its radius. So the bubble sizing is limited to the detection of its resonance frequency. The principle is to insonify the bubble by two ultrasound waves : an high frequency imaging wave, f_i, which is chosen higher than the theoretical bubble resonance frequency in order to have a good resolution in space; a "pump" low frequency wave, f_p, which is closed to the bubble resonance frequency. The oscillation of the bubble will modulate the backscattered imaging wave. Chapelon showed that the interaction at $f_i \pm f_p$ between the two waves, due to the bubble nonlinear behaviour, is maximum when $f_p = f_r$. Leigthon considered this technique reliable but the main drawback is that the apparatus is not simple.

Let us consider the case where the bubble detection has to be done on a diver. This fact gives different constraints on the future application. For example the apparatus must be simple (the minimum of complexity in the setup, just what is needed). The aim is to realize detection and sizing but without any analog filters or amplifiers. Another restriction is that this measure has to be applied on a human body, so the maximum pressure sent has to be limited in order to guaranty the diver's safety. This is particularly the case when human tissue and blood are saturated with gas [16]. Another reason which leads Leighton to say that this method is not simple, is the necessity of three transducers: one for the "pump" wave and two for emitting and receiving the "imaging" wave. Cathignol proposes a pulsed method that could be applicable for our future application [17].

In this study, we propose to take into account the pulsed method developped by Cathignol and the constraint related to a measure *in situ*, *i.e.* to characterize bubbles with a very short time (in our case less than $0.1s$) and with a low level of pressure (according to the limitation in saturated tissues [16]). The last important thing is that the size of the bubble is not known before the measure, so a large range of frequencies has to be tested.

3 Experiments

3.1 Experimental system

The experimental setup developed [18] is depicted in Figure 1. The experiments were performed in a 2m $\times$ 3m water tank in order to decrease the effect of a potential standing waves due to the low frequency. The fabrication of microbubbles is made by a Braun OralB ® hydrojet. It creates a lot of bubbles whose the size varies between 20 μm and 200 μm. For the experiments, only one bubble is isolated on a wire of 80 μm-diameter. The benefit to use a single stationary bubble is that different techniques can be tested on the same bubble and so the results are comparable. The bubble size is controlled by a CCD camera. A couple of 1 MHz-frequency transducers (Imasonic®, f = 90 mm) are used to emit and receive the imaging wave. These transduc-

ers are arranged to have an ultrasound focusing in the same volume. To activate the bubble, a low frequency transducer is used (Ultran®, GMP, 50kHz). The two emitting transducers are connected to an arbitrary waveform generator (LeCroy®, ArbStudio 1104). The receiver transducer is connected to an numerical oscilloscope (Agilent Technologies®, InfiniiVision DSO5014A). All the instruments are piloted by a computer *via* a Labview® program.

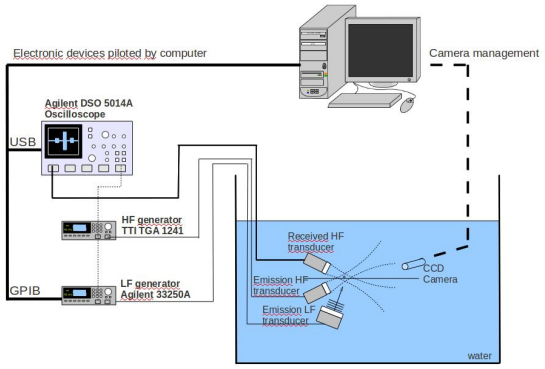

Figure 1: Experimental setup for bubble detection and sizing.

The "imaging" wave frequency f_i is always at 1 MHz. For these experiments, the Pulsed Repetition Frequency (PRF) is chosen between 1 kHz and 20 kHz and the duty cycle varies in function of PRF. The "pump" wave frequency has been chosen in order to size bubbles with radii between 55 μm and 110 μm. Considering the equivalent resonance frequencies, the "pump" frequency is swept automatically from 30 kHz to 60 kHz with a duration of 10 ms. This wave is sent ten times (total duration 100 ms). Amplitudes of emitted signals, high and low frequencies, are 12 V_{pp}. The corresponding acoustic pressure, measured on the focal point with an hydrophone (RESON®, TC4035), are 10 kPa for the "imaging" wave and 20 kPa for the "pump" wave. The received signal is recorded by a Labview® programm and then is treated on Matlab®.
The use of two high frequency transducers, one in emission and one in reception, is explained by different parameter sets which have been tested during experiments. Indeed in some cases, emission and reception can't be done on the same transducer.

4 Results

The received signal is treated with a Matlab® program. The aim is to detect the maximum of interaction at $f_i \pm f_p$ and the correspondent frequency of this maximum. According to the theory [17], the calculus of the FFT (Fast Fourrier Transform) of the entire beat signal shows an interaction but the automatic detection is difficult because of all the spectral lines at $f_i \pm n \times f_r$. The idea is to treat separately each received pulse. For each one, the signal is demodulated by multiplication with the emitted signal. Then the FFT of the pulse is calculated. By assembling all the calculated FFT, a spectrogram can be built. The spectrogram of three different beat signals with f_i = 1 MHz and $f_p \in [30\text{ kHz}; 60\text{ kHz}]$ and 25%-duty-cycle are shown on Figure 2. The difference between this three spectrograms is the repetition frequency that is equal to 2 kHz, 5 kHz and 10 kHz.

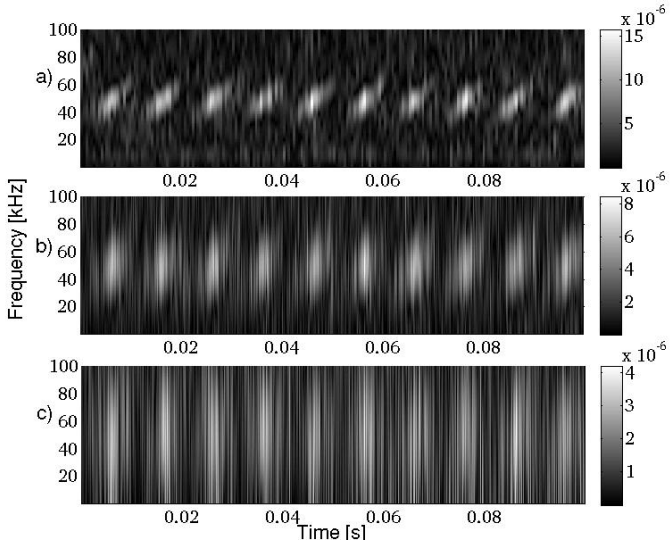

Figure 2: Reconstruction of 3 spectrograms from 3 different experimental beat signals with PRF of a) 2 kHz, b) 5 kHz and c) 10 kHz.

At this step of the detection, the goal is to detect the maximum of the demodulated signal for each sweep. Indeed the maximum of the spectrum is located at the bubble's resonance frequency. Two methods for the determination of the maximum are detailled.

4.1 Time-averaged

The first technique to detect the maximum of the spectrogram is to calculate the average of the reconstructed FFT. The result of this calculus will give a interaction curve in relation with the excitation frequency. The maximum of this curve is the interaction maximum and the corresponding frequency is the resonance one. The interaction curves for the three experimental beat signals are shown on Figure 3. The difference between this 3 curves is the repetition frequency that is respectively equal to 2 kHz, 5 kHz and 10 kHz. The measurements have been done on the same bubble but not in the same time so the bubble radius could have decrease because of rectified diffusion [19]. The maxima are situated at the same frequency (48 kHz) which corresponds to the bubble size measured at 67 μm. Measurements are accorded with the theoretical resonance frequency. The important result when the detection is done by this mean is that more the repetition frequency is high more the echo is short and more the interaction band is large. So when the repetition frequency increases the measurement quality decreases. Moreover, the main characteristic of a sweep in time is not completely used in this treatment.

4.2 Sweep discretisation

For one sweep, the frequency information can be directly read on the frequency scale but also on the time scale. Indeed the time scale is associated to the frequency one because the excitation frequency is linearly function of time. So the maximum of interaction is not anywhere on the spectrogram, it should be exactly on a line starting for a sweep at

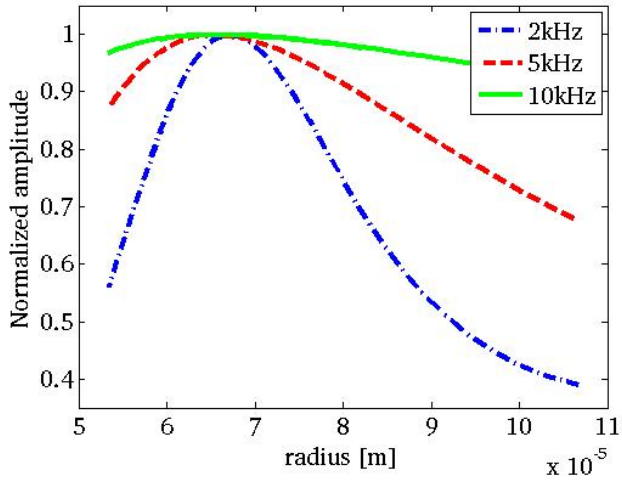

Figure 3: Representation of bubble sizing for three different signals by meaning the spectrogram on time. Respectively f_r = 2 kHz, f_r = 5 kHz and f_r = 10 kHz with a duty cycle of 25%.

30 kHz and finishing at 60 kHz (excitation sweep). Here the idea is to detect for each echo the maximum of interaction closed to the theoretical sweep. Then the detected maxima are recorded in a *n*-by-*m* matrix, where *n* is the number of echoes in one sweep and *m* is the number of sweeps. The representation of this matrix is given Figure 4 for the three different experimental beat signals with f_r equal to 2 kHz, 5 kHz and 10 kHz. The 10 sweeps are represented in the horizontal scale and for each, the vertical scale represented each echo.

For example in the third column, each line correspond to the maximum of the beat signal's FFT of one echo. The matrix mean on the 10 sweeps give a interaction curve in relationship to the excitation frequency. These curves are represented on Figure 5. The maxima are detected at 48 kHz, 49 kHz and 49 kHz. Theses frequencies correspond to bubble radii of 67 μm, 65 μm and 65 μm. Theses values are also accorded with the resonance frequency equation [20] with the consideration that the bubble could decrease during the measurements. The principal advantage of this method is the detection quality is not depending on the repetition frequency. Moreover this measure is equivalent for the three tested repetition frequencies (2 kHz, 5 kHz and 10 kHz).

The comparison of the two methods shows that the detection of maxima by sweep discretization is more efficient that by simple time-average especially at high PRF. The methods may be used to follow the changes in size due to diffusion.

5 Discussions

The bubble size has been controled by a camera but the resolution of the camera is 2,3 μm. So the bubble can't be exactly sized only with the camera. Moreover this size varies with the time because of the bubble rectified diffusion in water. The little the bubble is the more diffusion have an impact on its radius. So the bubble size is precisely checked with the classical dual frequency technique [15, 18] just before and after the measurement. All the measures are also done quickly to limit the change in size of the bubble. Acquisitions are done each 3 seconds and are repeated 41 times. Figure 6

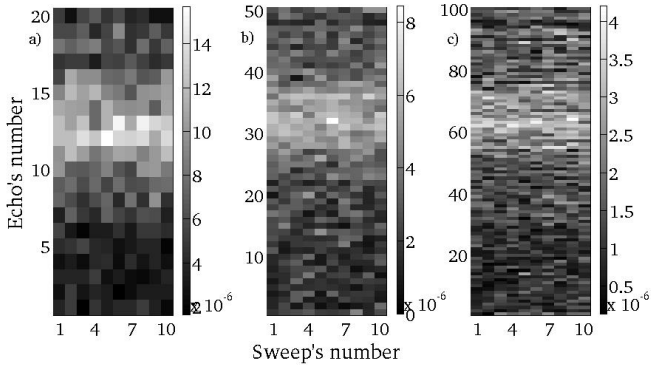

Figure 4: Maximum detection of the beat signal spectrum for each echo. The three PRF are a) f_r = 2 kHz, b) f_r = 5 kHz and c) f_r = 10 kHz.

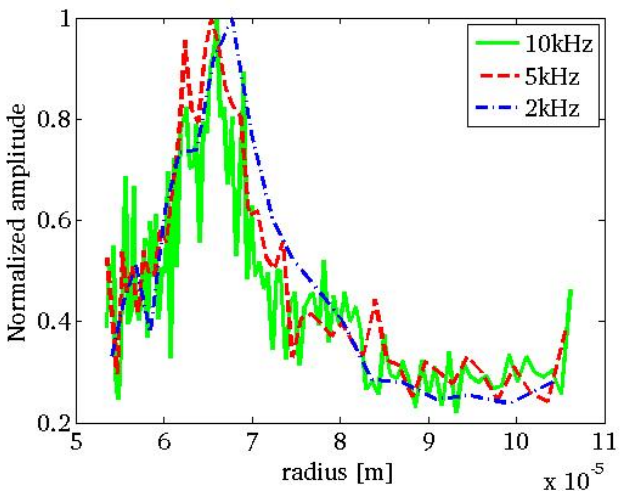

Figure 5: Representation of bubble sizing for three different signals by meaning the 10 sweeps. Respectively $f_r = 2kHz$, $f_r = 5kHz$ and $f_r = 10kHz$ with a duty cycle of 25%.

shows the measure done on a bubble. The controls are represented in continuous lines (green for the beginning and red for the end of the measure). The results of the first method are plotted in orange (triangular points) and the results of the second method are plotted in blue (square points).

The bubble sizing by the two developed methods is really accurate. A large number of bubbles have been sized several times for a total of almost 60 measures. The standard deviation can also be calculated between the experimental points and the mean of the two controls for every measurements. Moreover the maximum difference between the theoretical curves and the measurements is around 5% for the first method and 2.5% for the second one. An important detail is that these measures have been done with different set of parameters. Indeed the repetition frequency varies between 2 kHz and 20 kHz and the duty-cycle between 3% and 75%. The two determination methods of the bubble radius are efficient with a large range of repetition frequency. All the measurements done on a single bubble can also be represented on the same graph. Each point represents the mean of the 41 measures with the standard associated deviation. In Figure 7, the bubble size measurements during the rectified diffusion are represented.

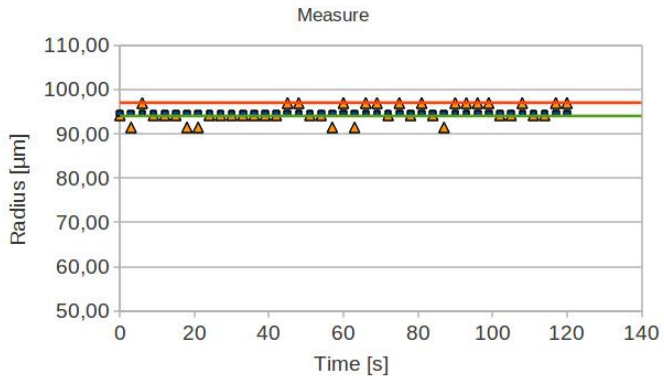

Figure 6: Bubble sizing by the pulsed bi-frequency method using two different treatments to detect resonance frequency.

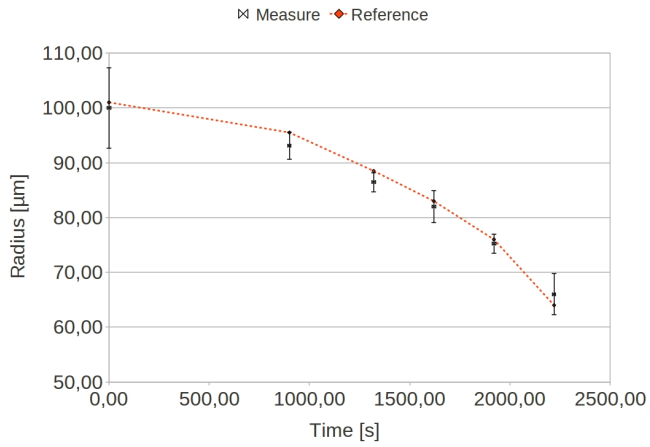

Figure 7: Measures of bubble diffusion in water.

6 Conclusion

The bubble can be sized precisely using a dual pulsed frequency method. Moreover the total detection time and the sending acoustic pressure are in good agreement with the constraint of an actual bubble detection in the right heart ventricular. The measures have been done on static microbubbles because it was necessary to be able to reproduce and to compare them. But now, an interesting test will be to size moving bubbles and to create an histogram of bubble population in acoustical field. An other limitation in these results is the low frequency transducer bandwidth. Indeed it is limited between 30 kHz and 60 kHz, so only bubbles with a radius between 55 μm and 110 μm can be sized. The feasibility of creating a low frequency with two different high frequencies is in progress.

Acknowledgments

This project has been carried out by BF SYSTEMES company in partnership with the LMA/CNRS under the sponsorship of French Ministry of Defense (DGA/Program RAPID - BORA).

References

[1] M. Cavaro, C. Payan, J. Moysan, and F. Baqu. Microbubble cloud characterization by nonlinear frequency mixing. 129(5):EL179–EL183, 2011.

[2] N. de Jong, F.J. Ten Cate, C.T. Lance, J.R.T.C. Roelandt, and N. Bom. Principles and recent developments in ultrasound contrast agents. *Ultrasonics*, 29(4):324 – 330, 1991.

[3] P.J.A. Frinking, A. Bouakaz, J. Kirkhorn, F. J. Ten Cate, and N. de Jong. Ultrasound contrast imaging: current and new potential methods. *Ultrasound in Medicine and Biology*, 26(6):965–975, 2000.

[4] A. Katiyar, K. Sarkar, and P. Jain. Effects of encapsulation elasticity on the stability of an encapsulated microbubble. *Journal of Colloid and Interface Science*, 336(2):519 – 525, 2009.

[5] D.E. Goertz, M.E. Frijlink, N. de Jong, and A.F.W. van der Steen. Nonlinear intravascular ultrasound contrast imaging. *Ultrasound in Medicine and Biology*, 32(4):491 – 502, 2006.

[6] G.J. Rubissow and R.S. Mackay. Ultrasonic imaging of in vivo bubbles in decompression sickness. *Ultrasonics*, 9(4):225 – 234, 1971.

[7] R.Y. and Nishi. Ultrasonic detection of bubbles with doppler flow transducers. *Ultrasonics*, 10(4):173 – 179, 1972.

[8] T. James Francis and S.J. Mitchell. Chapter 8 - pathophysiology of decompression sickness. pages 165 – 183, 2004.

[9] M.P. Spencer, S.D. Campbell, J.L. Sealey, F.C. Henry, and J. Lindbergh. Experiments on decompression bubbles in the circulation using ultrasonic and electromagnetic flowmeters. *Journal of Occupational Medicine*, 11:238, 1969.

[10] K. Kisman. Spectral analysis of doppler ultrasonic decompression data. *Ultrasonics*, 15(3):105 – 110, 1977.

[11] T.G. Leighton, A.D. Phelps, D.G. Ramble, and D.A. Sharpe. Comparison of the abilities of eight acoustic techniques to detect and size a single bubble. *Ultrasonics*, 34(6):661 – 667, 1996.

[12] D.L. Miller. Ultrasonic detection of resonant cavitation bubbles in a flow tube by their second-harmonic emissions. *Ultrasonics*, 19(5):217 – 224, 1981.

[13] T.G. Leighton, R.J. Lingard, A.J. Walton, and J.E. Field. Acoustic bubble sizing by combination of subharmonic emissions with imaging frequency. *Ultrasonics*, 29(4):319 – 323, 1991.

[14] T.G. Leighton, D.G. Ramble, and A.D. Phelps. The detection of tethered and rising bubbles using multiple acoustic techniques. *The Journal of the Acoustical Society of America*, 101(5):2626–2635, 1997.

[15] J.Y. Chapelon, P.M. Shankar, and V.L. Newhouse. Ultrasonic measurement of bubble cloud size profiles. *The Journal of the Acoustical Society of America*, 78(1):196–201, 1985.

[16] S.B Barnett, G.R Ter Haar, M.C Ziskin, H. Rott, F.A. Duck, and K. Maeda. International recommendations and guidelines for the safe use of diagnostic ultrasound in medicine. *Ultrasound in Medicine and Biology*, 26(3):355 – 366, 2000.

[17] D. Cathignol, J.Y. Chapelon, V.L. Newhouse, and P.M. Shankar. Bubble sizing with high spatial resolution. *IEEE transactions on ultrasinics ferroelectrics and frequency control*, 37(1):30–37, JAN 1990.

[18] T. Goursolle, B. Pottier, D. Fouan, and S. Mensah. Free single bubble ultrasonic detection : Chrip frequency excitations applied to nonlinear mixing method. In *Proceedings of the 44th Annual Scientific Meeting of UHMS*, Fort Worth, Texas, USA, June 2011.

[19] P.S. Epstein and M.S. Plesset. On the stability of gas bubbles in liquid-gas solutions. *The Journal of Chemical Physics*, 18(11):1505, 1950.

[20] F.D. Smith. On the destructive mechanical effect of the gas-bubbles liberated by the passage of intense sound through a liquid. *Philosophical Magazine*, 19:1147–1151, 1935.